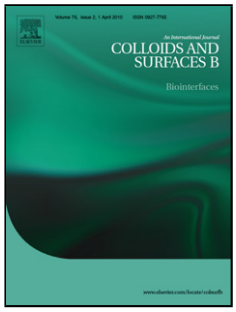

Title: An approach for liposome immobilization using sterically stabilized micelles (SSMs) as a precursor for Bio-layer Interferometry-based interaction studies

Author: Jakob Wallner Gabriele Lhota Markus Schosserer Karola Vorauer-Uhl

PII: S0927-7765(17)30133-9
DOI: http://dx.doi.org/doi:10.1016/j.colsurfb.2017.03.015
Reference: COLSUB 8425

To appear in: *Colloids and Surfaces B: Biointerfaces*

Received date: 29-11-2016
Revised date: 23-2-2017
Accepted date: 7-3-2017

Please cite this article as: J. Wallner, G. Lhota, M. Schosserer, K. Vorauer-Uhl, An approach for liposome immobilization using sterically stabilized micelles (SSMs) as a precursor for Bio-layer Interferometry-based interaction studies, *Colloids and Surfaces B: Biointerfaces* (2017), http://dx.doi.org/10.1016/j.colsurfb.2017.03.015

An approach for liposome immobilization using sterically stabilized micelles (SSMs) as a precursor for Bio-layer Interferometry-based interaction studies

Authors:

Jakob Wallner[a*], Gabriele Lhota[a], Markus Schosserer[a], Karola Vorauer-Uhl[a]

Address:

[a]Department of Biotechnology, University of Natural Resources and Life Sciences, Vienna
Muthgasse 11,
A -1190 Vienna, Austria

[*]Corresponding Author:

Jakob Wallner, Department of Biotechnology, University of Natural Resources and Life Sciences, Muthgasse 11, A-1190 Vienna, Austria.
E-mail: Jakob.Wallner@boku.ac.at
Phone: +43 -1 - 47654 - 79870
Fax: +43- 1 - 47654 - 79009

Statistical summary of the article:

total number of words: 6024

total number of tables: 3

total number of figures: 5

total number of Supplemental tables: 1

total number of Supplemental figures:1

Key words: Liposomes, protein/membrane interactions, Bio-Layer Interferometry, Octet, Biosensor, sterically stabilized micelles

Abbrevations used:

BLI, Bio-Layer Interferometry; BSA, Bovine serum albumin; cmc, critical micelle concentration; DLS, dynamic light scattering; DOPC, 1,2-dioleoyl-sn-glycero-3-phosphocholine; DPH, 1,6-Diphenyl-1,3,5-hexatriene; DPPC, 1,2-dipalmitoyl-*sn*-glycero-3-phosphocholine; DPPG, 1,2-dipalmitoyl-sn-glycero-3-phospho-(1'-rac-glycerol); DSPE-$PEG_{(2000)}$-biotin,1,2-distearoyl-*sn*-glycero-3-phosphoethanolamine-N-[biotinyl(polyethylene glycol)-2000] (ammonium salt); egg-PC, Egg Phosphatidylcholine; HSPC, soy L-α-phosphatidylcholine, hydrogenated; LDV, Laser Doppler Velocimetry; LOQ, Limit of quantification; MLV, multilamellar vesicle; NaCl, Sodium chloride; PEG, polyethylene glycol,; PBS, Phosphate-buffered Saline; PDI, polydispersity index; RSD, relative standard deviation ; R_t, specific response; SPR, Plasmon Resonance; SA, streptavidin, SSMs, sterically stabilized micelles; THF, Tetrahydrofuran; TOCL, Cardiolipin; ULV, unilamellar vesicle; ZP, Zeta potential

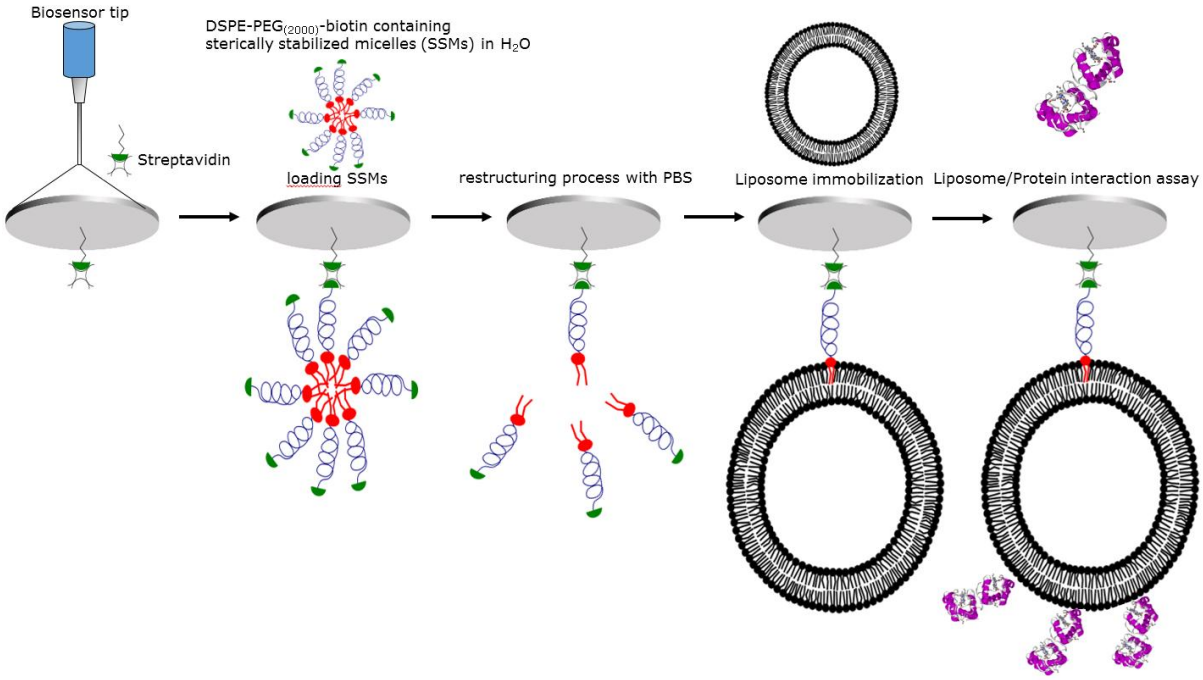

Abstract

Non-fluidic Bio-layer Interferometry (BLI) has rapidly become a standard tool for monitoring almost all biomolecular interactions in a label-free, real-time and high-throughput manner. High-efficiency screening methods which measure the kinetics of liposomes with a variety of compounds require the immobilization of liposomes. In this work, a method is described for immobilizing liposomes for interaction studies, based on the biophysical principles of this biosensor platform. The immobilization approach includes the loading of DSPE-PEG$_{(2000)}$-biotin containing sterically stabilized micelles (SSMs) which are restructured in a buffer change step, resulting in an accessible substrate for liposome immobilization. Liposomes in a concentration of 5 mM of varying composition and fluidity were immobilized on the sensor surface by inserting the hydrophobic residues of the former loaded SSMs. This proof of principle was carried out using Cytochrome C as a membrane-interacting model protein. The binding of Cytochrome C to the immobilized liposomes was demonstrated, and the derived kinetic and affinity constants were similar to values given in the literature. In order to obtain a detailed understanding of this surface, and to show the integrity of the liposomes, confocal fluorescence microscopy was used. Images of immobilized liposomes containing Calcein in the aqueous core indicated intact vesicles. A combination of this simple liposome immobilization approach, the possibility of automation on BLI systems with high throughput within an acceptable timescale and excellent reproducibility makes this assay suitable for basic research as well as for industrial and regulatory applications.

1. Introduction

The real-time kinetics of liposome/protein interactions is essential in the biological and biomedical sciences [1]. Liposomes, spherical nanostructures consisting of one or more phospholipid bilayers enclosing an inner aqueous compartment, can be used in numerous applications [2] [3]. As membrane models, liposomes are suitable not only for the study of lipid interactions with proteins, peptides and small molecules but also for the reconstitution of membrane proteins [4]. Liposomes can also be used as drug carriers for human applications such as anti-cancer therapeutics, signal enhancers in diagnostics and as adjuvants in vaccination [5]. In this case, drug kinetics can predict their bioavailability, triggered by interaction with blood proteins and for process development [6]. Meanwhile, various label-free fluidic and non-fluidic techniques to measure liposome/protein interactions have been established [7] [8]. The applications for biosensor-based fluidic systems such as surface plasmon resonance (SPR) are limited due to the fact that liposome suspensions and/or crude samples from different origins may clog the capillaries or enhance aggregation effects [9]. In the current work, we use the non-fluidic bio-layer interferometry (BLI) platform equipped with a shaking micro-well plate, enabling full kinetic measurements of crude and complex samples. We have already previously demonstrated that a BLI technique using disposable optical-fibre biosensors is in principle appropriate for the analysis of liposome/protein interactions [7]. This work has been well recognized, although the assay performance is subject to several limitations for instance that the protein of interest needs to be coated on appropriate sensors. This assumes that the protein of interest is in principle a membrane-interacting protein; furthermore, it needs to be labelled prior to coating, which is not only time-consuming but more importantly may alter the protein structure, inhibiting

the liposome binding. Additionally, this approach is not convenient for multimeric protein complexes which are formed in solution.

An improved, generally applicable concept is therefore required, utilizing an anchor which is different from the molecule of interest. This approach should: (i) be applicable for various liposomal compositions; (ii) enable measurement of non-specific binding; (iii) be appropriate for the measurement of membrane/protein kinetics; and (iv) allow the development of a high-throughput tool box. Based on the fact that freely accessible hydrophobic alkyl chains of phospholipids are able to spontaneously interact with lipid bilayers through hydrophobic interactions, a biotinylated polyethylene glycol lipid is used here, namely DSPE-$PEG_{(2000)}$-biotin [10]. However, the required accessibility in aqueous solutions is restricted, due to the hydrophobic effects of this amphiphilic molecule. Above the critical micelle concentration (CMC), sterically stabilized micelles (SSMs) will be formed. Below the CMC, monomers will adsorb preferentially at the air–water interface, leading to insufficient loading on the biosensor surface [11]. The fact that the structural and dynamic properties of SSMs strongly depend on environmental conditions can be utilized for (i) the formation of SSMs with a low aggregation number (~8 monomers); (ii) sufficient loading; (iii) specific disruption of the micellar structure by buffer changes; and (iv) creating accessible alkyl chains [12]. The functionality of this anchor is successfully verified by the immobilization of various liposome formulations. Their integrity was studied using fluorescence microscopy and Cytochrome C kinetics as model [13]. In addition, non-specific binding was evaluated with BSA. To the best of our knowledge, this simple approach has never before been used to immobilize liposomes on a biosensor.

2. Materials and Methods

2.1 Reagents

1,2-dipalmitoyl-sn-glycero-3-phosphocholine (DPPC), 1,2-dioleoyl-sn-glycero-3-phosphocholine (DOPC), soy L-α-phosphatidylcholine, hydrogenated (HSPC), Cardiolipin (TOCL), 1,2-dipalmitoyl-sn-glycero-3-phospho-(1'-rac-glycerol) (DPPG), 1,2-distearoyl-*sn*-glycero-3-phosphoethanolamine-N-[biotinyl(polyethylene glycol)-2000] (ammonium salt) (DSPE-$PEG_{(2000)}$-biotin) and Cholesterol were purchased from Avanti Polar Lipids (Alabaster, Alabama, USA). Egg Phosphatidylcholine (egg-PC) and 1, 2-distearoyl-sn-glycero-3-phosphoethanolamine-N-[amino(polyethylene-glycol)-2000] (DSPE-$PEG_{(2000)}$) were kindly provided by Lipoid (Ludwigshafen, Germany). Chloroform and sodium chloride (Merck, Vienna, Austria) was used in analytical grade quality. Phosphate buffered saline (PBS) was obtained from PAA (Pasching, Austria). The phosphate buffer saline (PBS) contained 137 mM NaCl, 2.7 mM KCl, 10 mM Na_2HPO_4 , and 1.8 mM KH_2PO_4, adjusted at pH 7.4.Ultra-pure water (resistance 18 MΩ/cm2) was produced with Ultra Clear UV (Evoqua Water Technologies LLC, Barsbüttel, Germany). 1,6-Diphenyl-1,3,5-hexatriene (DPH), Tetrahydrofuran (THF), Bovine serum albumin (BSA) and Calcein in analytical grade were received from Sigma Aldrich.

2.2 Liposome preparation

Multilamellar liposomes (MLVs) were prepared by the classical film rehydration method [14]. Different liposome formulations, which cover a wide range of biological and industrial application examples and possess different headgroups and lipid bilayer phase behavior were used (Table 1) [15] [6] [16]. Therefore, eight different liposome formulations were prepared consisting of either pure DPPC, pure DOPC,

DOPC:Cardiolipin (70:30 mol %) pure HSPC, HSPC:Chol (60:40 mol %), HSPC:Chol:DSPE-$PEG_{(2000)}$ (55:45:5 mol %), pure DPPG and pure egg PC. The individual lipids, in a total lipid concentration of 20 mM, were dissolved in 5 ml chloroform, evaporated in a rotating round bottom flask at 50 °C in a water bath at reduced pressure until a dried lipid film was generated. Each film was rehydrated in 5 ml PBS at 50 °C. For Calcein encapsulation, DPPC lipid film was reconstituted with 1 mM Calceinsolution in PBS, pH 7.4. Unilamellar vesicles were prepared by downsizing the MLVs by extrusion through 400, 200, and finally 100 nm polycarbonate membranes at 50 °C. For downsizing of the preformed liposomes an extruder from Avestin (Mannheim, Germany), equipped with polycarbonate Whatman membranes with different cut-offs of 400, 200 and 100 nm (GE Healthcare, Vienna, Austria), was used. Extrusion was performed 6 times through 400 and 200 nm and 10 times through 100 nm membranes at a working pressure between 2 and 30 bar [17]. For DPH-labeled liposomes a 3 mM DPH stock solution in THF was prepared. The stock solution was diluted 1:100 with PBS. This aqueous solution was added to the preformed DPPC liposomes to reach a final probe-to-lipid ratio of 1:200 and incubated at room temperature for 30 min. Unentrapped Calcein and not incorporated DPH were removed by gel fitration with PD-10 Desalting Columns (GE Healthcare, Vienna, Austria).

193 **Table 1**

194 Applied liposome formulations, lipid ratio, lengths of carbon chains, saturation, lipid

195 bilayer phase behavior and application examples.

Lipid	Molar ratio mM	Number of carbons: Number of double bonds	Transition temperature or lipid phase [18]	Application
DOPC	20	18:1	–16.5 °C	**a, b**
DOPC/TOCL	14:6	18:1 (DOPC) 18:1 (TOCL)	< 0 °C	**a, b**
egg-PC (major constituent POPC)	20	16:0 (33% POPC) 18:1 (31% POPC) 18:2 (15%) 18:0 (13%)	< 0 °C	**a, b**
DPPC	20	16:0 (DPPC)	41.3 °C	**a, b**
DPPG	20	16:0 (DPPG)	41.0 °C	**a, b**
HSPC	20	18:0 (88.6%) (HSPC) 16:0 (11.4)	~ 53 °C	**b**
HSPC/Chol	12:8	18:0 (88.6%) (HSPC) 16:0 (11.4) (HSPC)	Liquid ordered phase	**c, d**
HSPC/Chol/ DSPE-PEG$_{(2000)}$	11:8:1	18:0 (88.6%) (HSPC) 16:0 (11.4) (HSPC) 18:0 (DSPE-PEG$_{(2000)}$)	Liquid ordered phase	**c**

196

197 **a** : artificial cellular membranes

198 **b** : clinically approved liposome formulation component

199 **c** : clinically approved liposome formulation

200 **d** : mimicking lipid rafts

201

202

203

204

2.3 Size and homogeneity

The liposome mean diameter and the homogeneity were measured by DLS (Dynamic light scattering) with a Zetasizer Nano-ZS with software version 7.03 (Malvern Instruments, Malvern, UK) at 25 °C. Liposomal suspensions were diluted 100-fold with double distilled water prior the measurement. Each suspension was measured in five replicates. Size distribution was calculated by the intensity report. The homogeneity of the liposomes was determined by the polydispersity index (PDI).

2.4 Zeta potential

The zeta potential of Liposomes was determined by Laser Doppler Velocimetry (LDV) with the Zetasizer Nano-ZS with software version 7.03 (Malvern Instruments, Malvern, UK) at 25 °C. Samples were diluted 50-fold with 0.2 µm filtered PBS buffer for the analysis and were measured five times.

2.5 Biolayer Interferometry (BLI)

Octet QK (ForteBio, Menlo Park, CA, USA) was used for binding studies. Assay performance is shown in Fig. 1. Samples were diluted in black 96 well plates (Nunc F96 MicroWell™ Plates, Thermo Fisher Scientific, Langenselbold, Germany). The total working volume for each sample or buffer was 0.21 ml per well and the rpm setting for each equilibrium, loading, association and dissociation step was 1000 rpm. The test was performed at 30 °C. Prior each assay, streptavidin (SA) biosensor tips (ForteBio, Menlo Park, CA, USA) were pre-wetted in 0.21 ml PBS for at least 10 min followed by equilibration with PBS for 60 s (s = seconds). Afterwards, SA

biosensor tips were non-covalently loaded with SSMs in a concentration of 100 µg/ml (33µM) in ultra-pure water for 150 s, followed by an additional equilibration step (60 s) in PBS. Subsequently, the individual liposome formulations in a concentration of 5.0 mM in PBS or 500 mM NaCl in PBS, both pH 7.4 were immobilized for 800 s. A final washing step with PBS for 150 s was applied to remove unbound vesicles. Prior to the Cytochrome C association a blocking step with BSA (1mg/ml) for 300 s was introduced followed by another washing step with PBS for 100 s. Association of Cytochrome C in a concentration range of 100 µM, 50 µM, 30 µM and 5 µM to the immobilized DPPC (negative control)- and DPPG liposomes (positive control) was performed. Association for each concentration was carried out for 500 s. Finally, the dissociation was monitored with PBS for 500 s. All measurements were performed in triplicates.

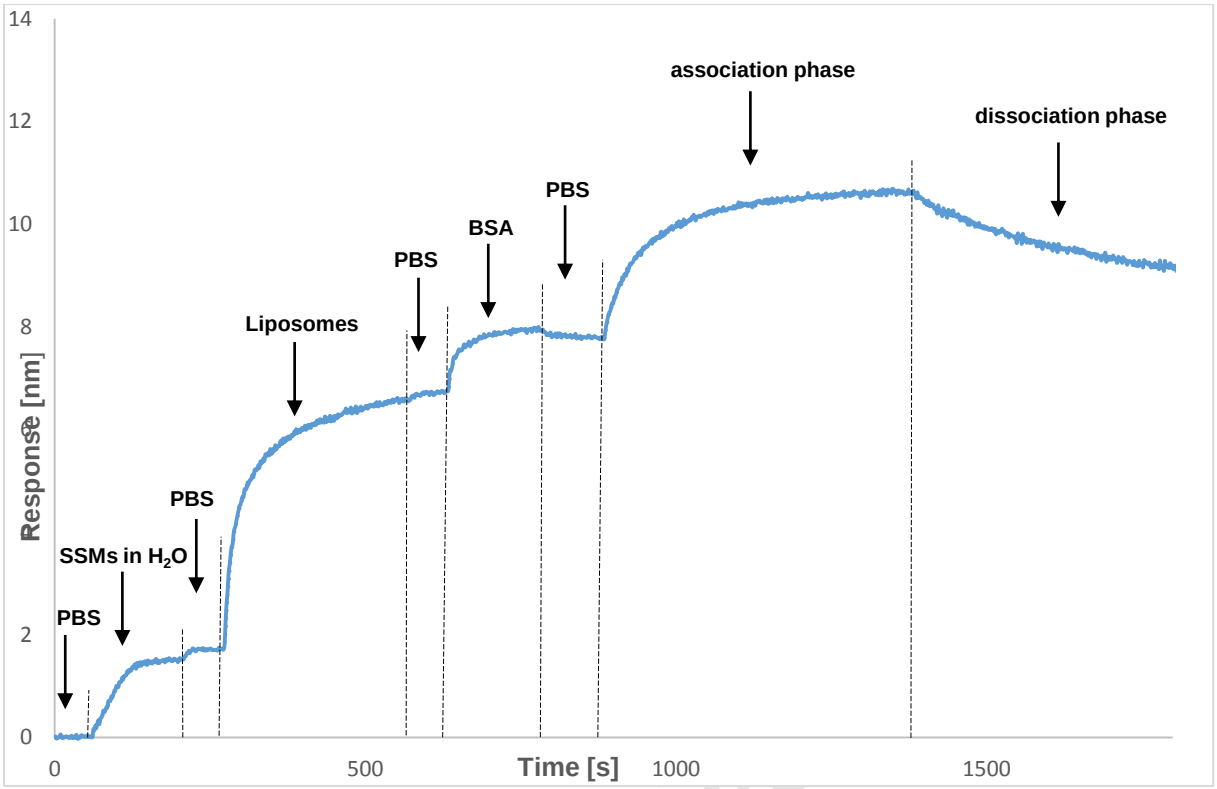

Fig. 1. Sensorgram of a typical test performance, including baseline steps, linker loading, liposome immobilization, BSA blocking step, protein association and dissociation.

2.6 Data analysis

Raw data, obtained with the Octet Software (Version 6.4, Menlo Park, CA, USA) were exported to Excel spreadsheets (Version 2003, Microsoft, Redmond, WA, USA). Raw data of the linker loading curves, the individual liposome immobilization curves and the Cytochrome C association and dissociation response were aligned to the individual association step. The individual specific response R at a defined time t (R_t) for each concentration was calculated as an average of three independent measurements. The reproducibility of R_t was determined with n=8. Interferometry data were globally fitted to a simple 1:1 Langmuir model calculating the affinities and rate constants (Octet software, Version 6.4, ForteBio) [7]. The fitted parameters were calculated as an average of three independent measurements. The association rate constant (k_a) is defined as the rate of complex formation per second in a 1 molar solution of two reaction partners. The dissociation rate constant (k_d) indicates the stability of this complex. However, the k_d can only be calculated if a decay in the signal of 5% or more is observed as described by Katsamba et al. [19].
That implies if the dissociation phase shows less than a 5% decrease in signal during the defined dissociation phase, as observed for the liposome immobilization step, a precise determination of the dissociation rate constant (k_d) is not possible [20] . However, it is feasible to calculate an upper limit for the individual affinities of the liposomes. Instead of precise affinities we calculated apparent affinity constants. Hence, for liposomes dissociation rate constant (k_d), the k_d (s^{-1}) is given by $k_d < -\ln(0.95)/t_d$, where td is the amount of the dissociation time in seconds [21] [7]. The affinity constant K_D is calculated by the ratio of k_d/k_a.

The quantitation limit for Cytochrome C association was assumed by measuring the minimum concentration at which the analyte can be reliably quantified. A typical signal-to-noise ratio is 10:1.The baseline noise was determined during the initial 60 s PBS buffer step (n=8). The RSD was defined as the standard deviation divided by the mean and multiplied by 100.

2.7 Imaging

Immobilized DPPC vesicles were studied by upright fluorescence microscopy and confocal fluorescence microscopy. An upright fluorescence microscope DM5500B (Leica Microsystems, Wetzlar, Germany) equipped with the L5 filter cube (excitation filter: BP 480/40; dichromatic mirror: 505 and suppression filter: BP 527/30) was used. Imaging was carried out with Leica Application Suite Advanced Fluorescence V2.6.9.7266 (Leica Microsystems, Wetzlar, Germany). The biosensor tip was cut to obtain an approximately 10 mm slice and mounted with the coated surface facing upwards in a prefabricated polystyrene component. Brightness, contrast and image size were adjusted in Irfan View (Irfan Skiljan, Wiener Neustadt, Austria). For confocal fluorescence microscopy, after liposome immobilization, the probe was mounted with the coated tip facing downwards in a PBS-filled glass bottom dish (IBIDI, Martinsried, Germany) on the inverted stand of a Leica SP8 confocal microscope (Leica Microsystems, Wetzlar, Germany). Microscopic images were acquired with the following settings: HC PL APO CS2 20x/0.75 DRY objective, bidirectional scanning at 400 Hz with a supercontinuum pulsed visible light laser at 486 nm, detection with a hybrid detector (491 nm – 674 nm, time gating: 0.6 – 6.0 ns), 0.132 µm pixel size, 1.06 zoom, 56.6 µm pinhole (1.00 airy), frame average 3, line average 3. Confocal images were deconvolved in Huygens Professional

(Scientific Volume Imaging, Hilversum, Netherlands) using a calculated PSF, CMLE algorithm, SNR = 20, quality threshold = 0.05 and 40 iterations. Brightness, contrast and image size were adjusted in Irfan View (Irfan Skiljan, Wiener Neustadt, Austria). Through all acquisition and processing steps, sample and control images were treated exactly the same way.

3. Results and Discussion

3.1 Liposomes

BLI can be used to measure the increase of the thickness on the biosensor surface, since BLI directly correlates the spectral shift ($\Delta\lambda$) with the change in thickness (nm) [22].

For the proposed approach, it was necessary to ensure that the liposome preparations had the same mean size and a low polydispersity, indicating a homogeneous distribution; in this way, the immobilization of various liposomes with the DSPE-$PEG_{(2000)}$-biotin linker can be related to the lipid composition. Furthermore, the comparison between the interactions of DPPC and DPPG liposomes with Cytochrome C is more reliable when using liposomes with the same mean sizes. Another important issue was to ensure that the 500 mM NaCl/PBS did not affect the stability or polydispersity due to the osmotic difference between the external and internal solutes. The quality of the preparations was therefore determined using DLS, and the mean diameter and homogeneity were calculated. All liposomes, regardless of suspended in PBS or 500 mM NaCl/PBS, had a mean size of 90±10 nm; the

calculated polydispersity index (PDI) indicated that all liposomes were homogeneously distributed and remained stable in NaCl (Supplemental Table 1).

3.2 Zeta potential

In other biosensor-based techniques, the immobilization of anionic liposomes in low ionic strength buffer (PBS) is essentially impossible [23]. In this study, we aim to demonstrate the effect of liposome surface charge on the linker capture immobilized on the tips of the SA biosensor.

Slightly negative zeta potential values were determined for zwitterionic DOPC, DPPC, HSPC, HSPC/Chol and HSPC/Chol/DPSE-PEG_{2000} liposome formulations, in the range −4.36 to −0.78 mV. The zeta potential of egg PC liposomes showed an approximately neutral value of +0.1 mV. Anionic DPPG and a mixture of zwitterionic DOPC and anionic TOCL liposomes showed strongly negative zeta potentials of −36.7 and −21.0 mV respectively (Supplemental Table 1). Zeta potential measurements were only carried out in PBS, since 500 mM NaCl/PBS has high conductivity, and this is unreliable for ZP measurements according to the manufacturer's recommendations.

3.3 BLI Assay Process

A typical BLI assay involves four essential steps: an equilibrium step, immobilization of the ligand, association of the analyte and a dissociation step. To adapt this technology for liposome/protein interaction analysis, the assay process was modified. For an appropriate liposome-based assay, an additional step is required involving the attachment of the lipophilic anchor prior to the immobilization of the liposomes.

3.3.1 Step 1: Equilibration

The assay sequence begins with the equilibration of the SA biosensor tips with the PBS buffer in order to measure the baseline signal for calculation of the LOQ, which is defined as the lowest concentration at which the analyte can not only be reliably detected but at which some predefined goals for bias and imprecision are met. To obtain LOQ datasets for the evaluation of significant measurements, the average baseline noise was determined and the LOQ assumed to be a signal-to-noise ratio of 10:1 [24]. The baseline noise of the initial 60 s PBS buffer step was 0.04 nm (n=8).Thus, the LOQ was calculated as 0.4 nm.

3.3.2 *Step 2: Loading of Sterically Stabilized Micelles (SSM)*

In order to apply liposomes within a biosensor, two main strategies for immobilization have been developed. The first is based on lipophilic surface chemistry, such as the covalent linking of alkyl groups to the chip surface. These sensor chips and kits are

now commercially available. However, the applications of this approach are limited by certain drawbacks such as the risk of liposome structure rupture, incomplete surface regeneration and non-specific binding of analytes to the lipophilic surface in the following interaction analysis [25] [26]. The second strategy uses liposomes containing trace amounts of various tag-lipids. The most commonly used tag-lipids are biotinylated lipids, which can bind to immobilized streptavidin and must be added prior to liposome formation [27]. This technique has some limitations, since the amount of biotinylated lipid must be optimized for each liposome formulation, an appropriate spacer between the biotin and the functional group of the lipid needs to be optimized and membrane properties may be altered [16].

Although different manufacturers offer sensor-chip-based platforms, no biosensor tips with long chain lipophilic groups attached on the surface are commercially available for the BLI approach. However, SA biosensor tips are commercially available, among others, which can be used in BLI for the immobilization of liposomes if an appropriate anchor system is established. Thus, the goal of this study is to identify a lipophilic anchor that is able to capture various liposome formulations. A biotinylated lipid was therefore used and tethered to the SA biosensor surface, which facilitates post insertion into liposomes [28]. Although the biotin-streptavidin bond is known to be one of the strongest non-covalent biological interactions, and very rapidly forms stable complexes at a wide range of pH and temperature, a major challenge is the attachment of biotinylated lipids in a site-directed configuration due to hydrophobic effects [29]. Thus, the development of an immobilization procedure for biotinylated lipids as an anchor is crucial. The introduction of hydrophilic PEG chains, which are also available with biotin, increases the water solubility. Thus, aqueous systems can be used and biosensor

non-compatible organic solvents can be avoided. Additionally, PEG chains inhibit the spreading of liposomes on a surface [30]. However, the amphiphilic character of the PEGylated lipid is conserved and will lead to micelle formation above the critical micelle concentration (CMC), which prevents incorporation into the preformed liposomes. A working range of concentrations below the CMC is suboptimal for sufficient loading due to monomer adsorption at the air-water interface, and initial attempts to immobilize liposomes failed (preliminary data not shown). As described above, DSPE-$PEG_{(2000)}$ lipids form sterically stabilized micelles whose structural and dynamical properties strongly depend on the solvent medium [31] [32]. The critical micelle concentration is approximately 10–25 µM in water, about 10 times higher than in an isotonic buffer (0.5–10 µM), and even more importantly, their aggregation number differs. Micelles assembled in water consist of about 8 monomers, whereas in PBS the aggregation number increases up to approximately 90 monomers. Furthermore, in micelles with a lower aggregation number, a large fraction (~30%) of the hydrophobic core is fully exposed to water, resulting in micelle destabilization. In contrast, less than 10% of the core of the larger micelles is exposed to PBS, indicating greater thermodynamic stability compared with micelles in water [12]. After the loading of SSMs in water, a buffer wash step (PBS) was introduced (100 s). This resulted in a dissociation of monomers from micelles not bound to streptavidin. SSMs in a monomer concentration of 100 µg/ml (33 µM) were loaded to the equilibrium state (1.1 and 1.3 nm), as shown in Supplemental Fig. 1.

440
441
442

443 3.3.3 *Step 3: Immobilization of Liposomes*

444 The SSM-coated SA biosensor tips were incubated with various liposomes at
445 concentrations of 5 mM to measure the corresponding immobilization profiles of
446 DPPC, DPPG, DOPC, DOPC/Chol, egg-PC, HSPC, HSPC/Chol and
447 HSPC/Chol/DSPE-$PEG_{(2000)}$, diluted in PBS (Fig. 2A) or 500 mM NaCl/PBS (Fig 2B).

448
449
450
451
452
453
454
455
456
457
458

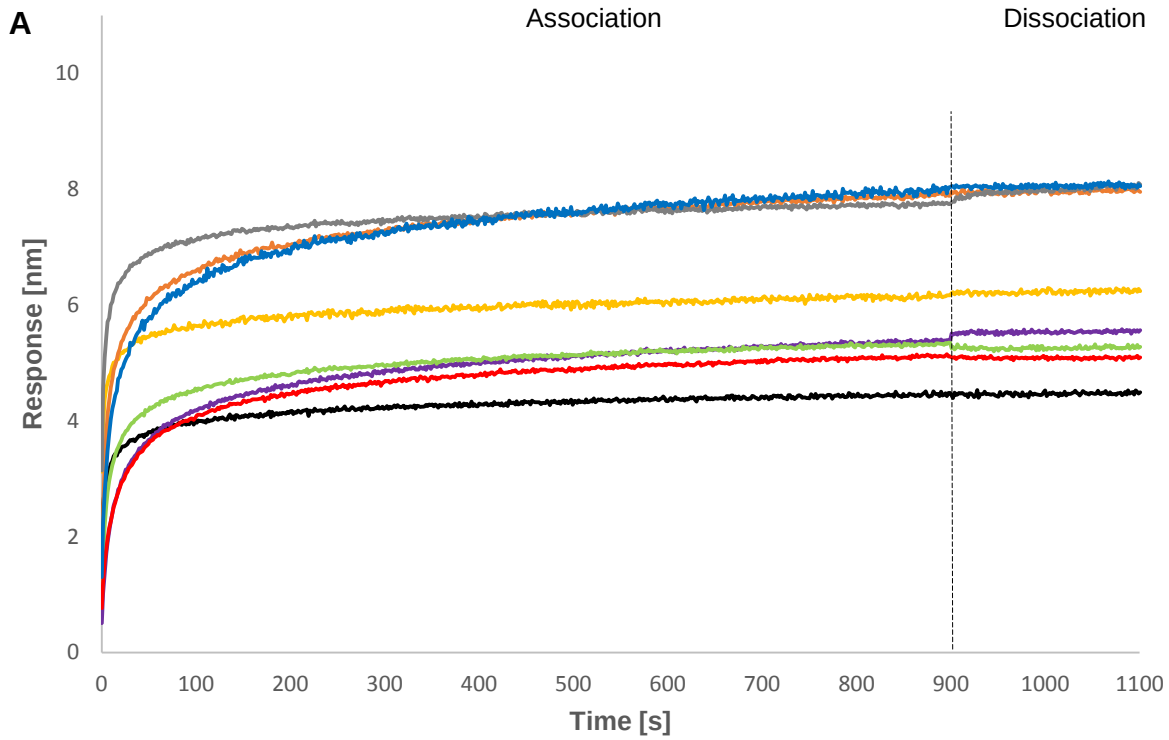

459

460

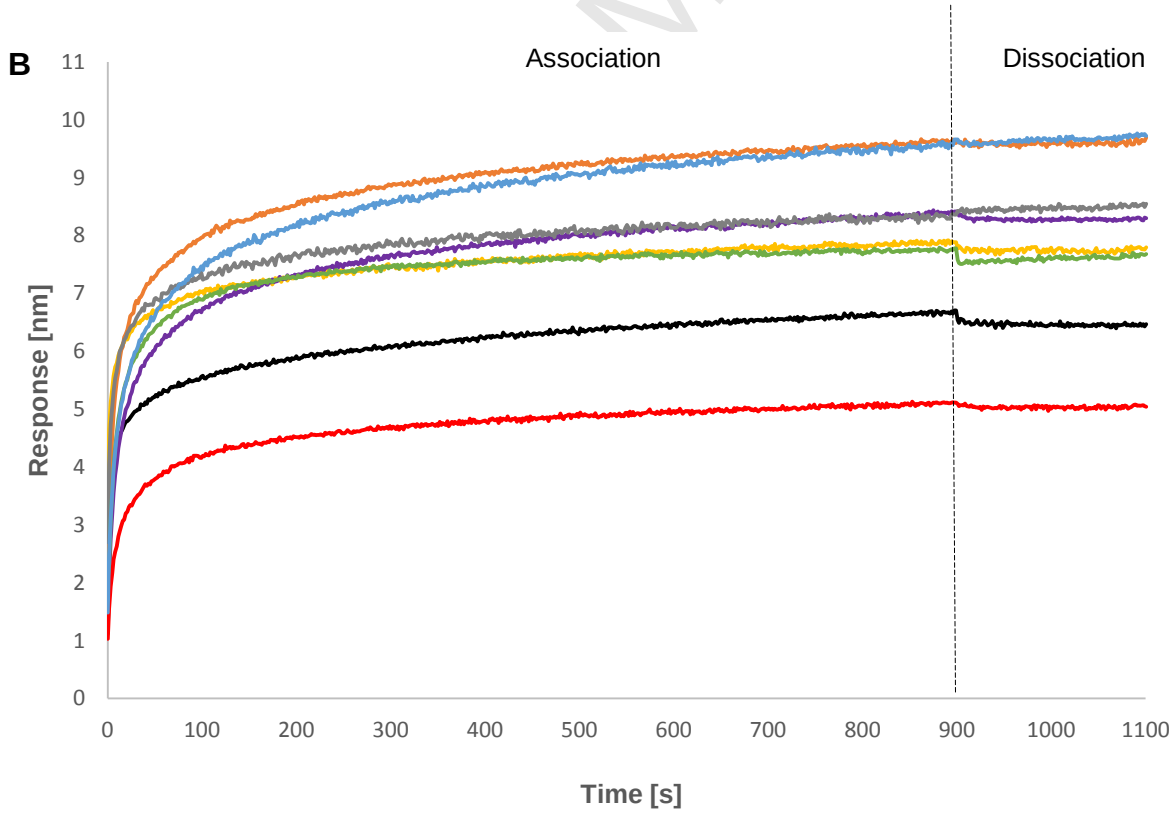

461

462

DOPC DOPC/Cardiolipin DPPC DPPG egg PC HSPC/Chol HSPC/Chol/PEG HSPC

Fig. 2: Liposome immobilization and dissociation curves of DOPC, DOPC/Cardiolipin, DPPC, HSPC, DPPG, egg-PC, HSPC/Chol, HSPC/Chol/$PEG_{(2000)}$ diluted in PBS (A) or 500 mM NaCl/PBS (B). The curves represent the mean values of triplicate measurements of 5 mM liposome suspensions. SSMs in a constant concentration of 33 µM were loaded prior to liposome immobilization

In the preliminary experiments, various concentrations were tested for each liposome formulation. The specific response (R_t) was measured with 5 mM of each liposome formulation diluted in PBS or 500 mM NaCl in PBS (Table 2), both pH 7.4. Higher concentrations did not result in higher values, thus indicating the saturation of the tip surface.

Table 2

Specific response (R_t), apparent kinetic rate constants (K_a, K_d) and apparent affinities (K_D) determined for liposome immobilization. Liposomes were diluted in PBS or 500 mM NaCl/PBS

Analyte	R_t (nm)	K_a ($M^{-1}s^{-1}$)	K_d (s^{-1})	K_D (mM)
DOPC[a]	6.17 (0.22)[c]	20.75 (0.77)[d]	< 3.34	< 160
DOPC/TOCL[a]	4.48 (0.23)[c]	16.45 (0.67)[d]	< 3.34	< 200
Egg-PC[a]	7.75 (0.27)[c]	20.31 (0.65)[d]	< 3.34	< 160
DPPC[a]	7.89 (0.35)[c]	6.29 (0.18)[d]	< 3.34	< 530
DPPG[a]	5.40 (0.15)[c]	4.33 (0.13)[d]	< 3.34	< 770
HSPC[a]	8.03 (0.20)[c]	5.13 (0.25)[d]	< 3.34	< 650
HSPC/Chol[a]	5.35 (0.28)[c]	9.22 (0.11)[d]	< 3.34	< 360
HSPC/Chol/$PEG_{(2000)}$[a]	5.11 (0.09)[c]	4.67 (0.17)[d]	< 3.34	< 720
DOPC[b]	7.88 (0.43)[c]	16.53 (0.64)[d]	< 3.34	< 200
DOPC/TOCL[b]	6.71 (0.26)[c]	10.19 (0.15)[d]	< 3.34	< 330
Egg-PC[b]	7.88 (0.40)[c]	8.11 (0.40)[d]	< 3.34	< 410
DPPC[b]	9.60 (0.41)[c]	6.00 (0.22)[d]	< 3.34	< 560
DPPG[b]	9.50 (0.29)[c]	4.99 (0.12)[d]	< 3.34	< 670
HSPC[b]	9.66 (0.36)[c]	4.52 (0.14)[d]	< 3.34	< 740
HSPC/Chol[b]	7.78 (0.19)[c]	10.34 (0.50)[d]	< 3.34	< 320
HSPC/Chol/$PEG_{(2000)}$[b]	5.12 (0.13)[c]	5.65 (0.20)[d]	< 3.34	< 590

[a] Liposomes diluted in PBS

[b] Liposomes diluted in 500 mM NaCl/PBS

[c] Mean and standard deviation for three independent experiments

[d] Full global fit (mean and standard deviation for three independent experiments).

Each selected liposome suspension interacted in a buffer-dependent but also lipid-dependent manner. The highest R_t value was 8.03 nm for HSPC liposomes (PBS) and the lowest 4.48 nm for DOPC/TOCL liposomes (PBS). As expected, anionic and PEG-modified liposomes (PBS) showed significant lower R_t values, and this is in agreement with the published data [6]. In the NaCl buffer, the highest R_t value was 9.66 nm for HSPC and the lowest 5.11 nm for HSPC/Chol/$PEG_{(2000)}$. The R_t values of anionic DPPG and DOPC/TOCL liposomes and zwitterionic liposomes in PBS, were significantly increased using 500 mM NaCl/PBS. However, electrostatic repulsion is completely shielded in PEG-containing liposomes which had the same R_t values in both buffer systems. These results demonstrate that zwitterionic and ionic headgroups significantly affect the immobilization of liposomes; however, this effect can be eliminated simply by optimizing the buffer system. Liposome immobilization was highly reproducible, as shown by the narrow standard deviation. Since the aim of this project is to cover a wide range of biologically and industrially relevant formulations, the kinetic rate constants and affinities dependent on the membrane fluidity are of great importance; both parameters were therefore calculated and are summarized in Table 2. The selected liposomes can be divided into three categories according to their membrane fluidity. All measurements were performed at 30°C, and thus the membranes of the liposomes are in different states of fluidity. Liposomes consisting of DOPC, DOPC/TOCL and egg-PC are in the liquid-crystalline and liquid-disordered phase, DPPC-, DPPG- and HSPC-containing liposomes are in the solid gel phase, and the HSPC/Chol and HSPC/Chol/ DSPE-$PEG_{(2000)}$ liposomes are in the liquid ordered phase [18]. Liposomes in the liquid-crystalline phase showed the fastest interaction, followed by the liquid-disordered phase liposomes and the solid gel phase liposomes. HSPC/Chol/$PEG_{(2000)}$ represents an exception due to the

stealth effect of PEG chains. This expected order is in accordance with fundamental studies and demonstrates that the lipophilic acyl chains are able to penetrate into the lipid core of the liposomes; this is only possible if the SSMs are disrupted and sufficient acyl chains are present [10]. Additionally, the formation of very stable complexes, as shown by the negligible level of dissociation, supports these findings. As described in the section materials and methods, the dissociation rate constants are < 3.34 for each formulation based on $K_d < -\ln(0.95)/t_d$. However, the rates of complex formation (K_a) differ, as shown in Table 2. Since K_d is constant for each formulation and the calculated affinity (K_D) is the ratio of K_d / K_a, the K_D values are primarily determined by the K_a values. These values were determined as apparent association rate constants (ka) for each liposome formulation in order to estimate the liposome binding property in dependence on the membrane fluidity. Due to the fact that the liposomes are stable attached to the anchor we did not observe enough decay of the binding signal during the defined dissociation time to determine a precise dissociation rate constant (kd) for these interactions. Therefore, we were constrained to apply the ‘‘5% rule’’ for the calculation, which is indicated by the term “apparent” and make no claim to provide precise affinities [20]. Thus, the insertion rate is ordered as follows: DOPC > DOPC/TOCL > egg-PC > HSPC/Chol>DPPC > HSPC/Chol/$PEG_{(2000)}$ > DPPG. This ordering is independent of the applied buffer, and demonstrates that the interaction is profoundly dominated by the individual membrane fluidity.

3.3.4 *Step 4: Cytochrome C Assay*

Prior the liposome/Cytochrome C interaction, the liposome-coated sensor was blocked with 1 mg/ml BSA to cover all non-specific binding sites. Without this blocking step, Cytochrome C may interact with the linker and/or free sensor (data not shown).

Different R_t values for unspecific BSA bindings (Fig. 3) towards DPPC and DPPG in PBS were obtained (1.10 nm and 0.87 nm respectively). BSA blank values, below the LOQ of 0.4 nm, were obtained for sensors coated with DPPC and DPPG liposomes diluted in 500 mM NaCl/PBS. These findings are essential for the following protein interaction studies, and there are therefore two possibilities for performing a reliable test configuration. One approach is the selection of a suitable buffer for optimal immobilization, and the second is to block the surface with BSA. Both are possible without interference with the interaction assay.

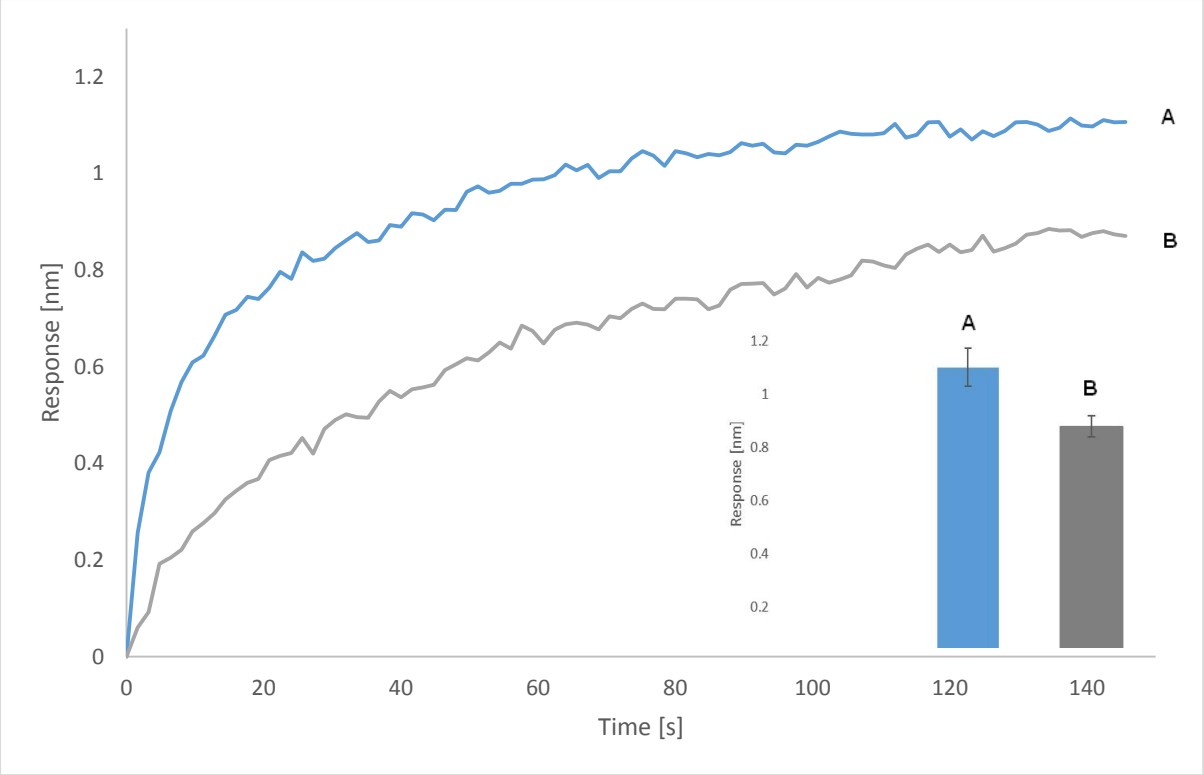

562

563

564 Fig. 3: BSA blocking curves for liposome-coated sensors with DPPG (A) and DPPC
565 (B). Liposomes were diluted in PBS. The curves represent the mean values of 12
566 independent measurements of 1 mg/ml BSA. The bars and error bars represent the
567 mean R_t values and standard deviation of 1 mg/ml BSA

568

569 To explore the functionality of the immobilized liposomes the well-established
570 liposome/protein interaction model of the interaction between anionic DPPG and
571 Cytochrome C was used, with DPPC liposomes as a negative control. These assays
572 were performed in PBS, while the liposome immobilization was performed in PBS or
573 NaCl; in each assay, a BSA blocking step was applied. As shown in Fig 4,
574 Cytochrome C interacted in a concentration-dependent but also in a lipid-dependent
575 manner.

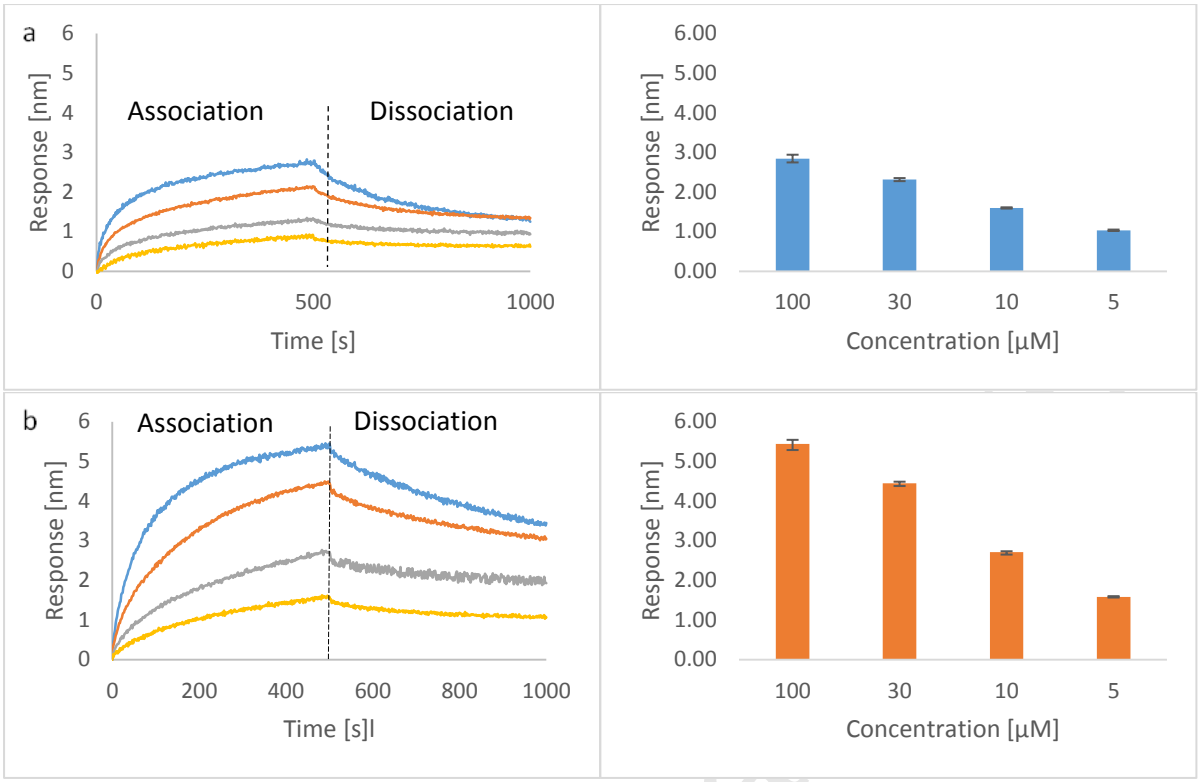

Fig. 4: Association and dissociation curves of Cytochrome C in a concentration range between 100 (blue), 30 (orange), 10 (grey) and 5 µM (yellow). SA biosensor tips were loaded with SSMs prior to liposome (a) DPPG/PBS (b) DPPG/ 500 mM NaCl/PBS immobilization. Liposome-coated sensors were blocked with BSA prior to Cytochrome C association. The curves represent the mean values of triplicate measurements of each concentration. Bars and error bars represent the mean R_t values and standard deviation for triplicate determinations of Cytochrome C association for concentrations of 100, 30, 10 and 5 µM to DPPG liposomes, diluted in PBS (blue) or in 500 mM NaCl/PBS (orange).

From the LOQ-based principle for reliable measurements, as explained in the materials and methods section, it was found that the mean R_t of Cytochrome C towards DPPC liposomes was significantly below the calculated threshold value of 0.4 nm (data not shown). The mean R_t values for Cytochrome C association, depending on the applied Cytochrome C concentration (5, 10, 30 and 100 µM) with DPPG liposomes (PBS) ranged between 1.03 nm and 2.84 nm. Sensors coated with DPPG liposomes in 500 mM NaCl/PBS were in the range 1.58 nm to 5.44 nm (Fig. 4). These results are in excellent agreement with published data and provide additional evidence that an improved efficacy of immobilization increases the sensitivity of the assay [33] [23] [13]. Full kinetic measurements including affinity and rate constants were calculated for the comparison of liposome/Cytochrome C binding under different experimental conditions as well as to compare our data with other methodologies.

Table 3 shows the calculated K_a, K_d, and K_D values. The calculated constants are in good agreement with values published with biosensor based techniques (SPR, BLI) [23] [33], whereas the DPPC liposome/Cytochrome C constants were not calculated since they failed the threshold criteria.

Table 3

Ligand	Analyte	K_a ($M^{-1}s^{-1}$)	K_d (s^{-1})	K_D (µM)
DPPG/PBS	CytC	195.6	1.48×10^{-3}	7.57 (0.34) (n=12)[a]
DPPG/NaCl	CytC	158.9	8.76×10^{-3}	5.51 (0.19) (n=12)[a]

Table 3: Kinetic rate constants and affinities determined for the liposome/Cytochrome C interactions

[a] Full global fit (mean and standard deviation for n-independent experiments)

The reproducibility of the test performance was evaluated with 30 µM Cytochrome C and immobilized DPPG liposomes in PBS (n=8). The corresponding R_t was 2.33 nm with a relative standard deviation (RSD) of 4.8%. The RSD (%) was defined as the standard deviation divided by the mean and multiplied by 100. These results demonstrate that the established assay is appropriate for liposome/protein interaction analysis.

3.4 Imaging

The configuration of the lipids on the biosensor surface profoundly affects the interaction of a protein or a peptide with the lipid layer. Hence, it is important to know whether the liposomes stay as intact vesicles on a biosensor or form a continuous, planar lipid layer. It is assumed that smooth hydrophobic surfaces promote the formation of planar lipid layers, whereas rough branched matrices facilitate the

immobilization of intact liposomes. According to the aim of our study, SSMs formed by biotinylated PEG lipids were used to immobilize intact liposomes. After binding to streptavidin, heterogeneous surface characteristics are created, and this should prevent the formation of smooth homogenous planar monolayers. In order to verify this, DPPC liposomes were imaged with upright and confocal fluorescence microscopy after immobilization. The lipid bilayer of the liposomes was stained with the hydrophobic membrane dye DPH, which intercalates spontaneously into membranes and is almost non-fluorescent in aqueous solution, whereas binding to the hydrophobic region of the membrane results in a strong fluorescence signal [34]. As expected, stained immobilized DPPC liposomes clearly showed a strong blue fluorescence signal (Fig. 5b), while dye-free immobilized DPPC liposomes did not (Fig. 5a). This result provides evidence for the immobilization of lipid bilayer systems; however, it provides no information about the integrity of the immobilized liposomes. Calcein, a water-soluble, membrane impermanent dye, was therefore encapsulated as an indicator for the topology of liposomes [35] [16]. Calcein self-quenches at concentrations above 70 mM, and a concentration of 1 mM was therefore used. Due to reflections of the blue incident light on the glass-fibre surfaces of the probe (data not shown), which completely obscured the specific green fluorescent signal, the upright fluorescence microscope could not be used. Thus confocal microscopy with a time-gated hybrid detector and a pulsed white-light laser was applied to circumvent this problem. Using this approach, most of the reflected light could be blocked out, and the presence of Calcein-stained liposomes was clearly detected (Fig. 5d). The presence of scratches on the coated tip (Fig. 5d), which were not visible in the control (Fig. 5c) further confirmed that the observed signal resulted from specific fluorescence and not from reflected light. The Leica SP8 confocal microscope has no

suitable excitation light source for the blue fluorescence dye DPH. It should also be mentioned that unentrapped dyes were removed by gel filtration, preventing any interference with microscopy. In conclusion, the DPH and Calcein fluorescence signals indicate that intact liposomes were immobilized on the SA tip by the pre-loaded SSMs.

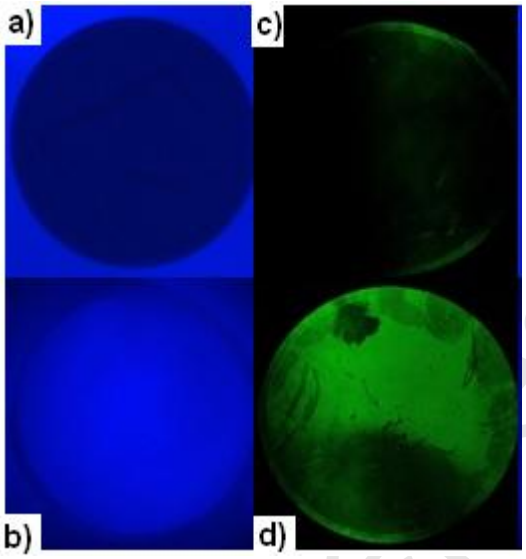

Fig. 5: Upright and fluorescence images of immobilized liposomes tethered to the former SSMs on a SA biosensor surface: (a) Fluorescence microscopy of unstained DPPC liposomes prepared in PBS; (b) Fluorescence microscopy of DPPC liposomes with the membrane dye DPH, (c) time-gated and deconvolved confocal microscopy image of unstained DPPC liposomes prepared in PBS; (d) time-gated and deconvolved confocal fluorescence microscopy image of DPPC liposomes prepared in PBS containing 5 mM Calcein. The water-soluble dye Calcein is enclosed in the

liposome lumen. Unentrapped dyes were removed by gel filtration. Representative images of three replicates are shown. The internal diameter of the biosensor is 600 µm (manufacturer's instructions).

4. Conclusion

In this work, we have demonstrated that sterically stabilized micelles (SSM) containing DSPE-PEG$_{(2000)}$ biotin with a low aggregation number can be used as a precursor to immobilize intact liposomes on a SA biosensor tip after simple buffer exchange.

This approach allows excellent liposome immobilization of various compositions and fluidities, including liposomes mimicking lipid rafts. Lower immobilization levels due to repulsion of ionic liposomes could be eliminated or compensated for using a high ionic strength buffer. Non-specific interactions of the protein of interest with the biosensor could be avoided or eliminated by introducing a blocking step. This proof-of-concept study of protein/liposome interaction measurements using BLI assay confirms that this technique is appropriate, in principle, for the analysis of protein/liposome interactions in a simple and reproducible manner. The results of the liposome/Cytochrome C assay demonstrate that the interaction between the protein and selected liposomes was strongly related to the biophysical properties of the liposome membranes. This well-established optical biosensor platform provides versatility in experimental design. In order to study the individual influence of various buffers or matrices, the microtiter plate system offers a method for rapidly exchanging the tested solvents; thus, liposome/protein interaction can be performed easily, in a high throughput manner and in an automated workflow. Additionally, the use of HTX-BLI based instruments in the 32-channel mode and 384 well plates

means that 32 individual real-time kinetic measurements of liposome/protein interactions can be performed during a single unattended run of less than 30 min. Finally, with minor specific optimizations, this approach can be adapted successfully for other analytical methods requiring the immobilization of hydrophobic anchors on surfaces and/or liposome immobilization. Future work will be carried out on the detailed characterization of the morphology of the liposomes immobilized on the sensor surface.

Conflict of interest

The authors declare that they have no conflicts of interest with the contents of this article.

Acknowledgments

The authors thank Sriram Kumaraswamy and Klaus Helm (ForteBio, Menlo Park, CA, USA) for kindly providing SA biosensor tips. We thank Monika Debreczeny (University of Natural Resources and Life Sciences Vienna, BOKU-VIBT Imaging Center, Austria) and Verena Ibl (University of Natural Resources and Life Sciences Vienna, IAGZ, Austria) for technical support with microscopy. We are also grateful for the gift of Egg Phosphatidylcholine from Lipoid GmbH (Ludwigshafen, Germany). Furthermore, we thank Dominik Jeschek (ACIB GmbH, Austrian Centre of Industrial Biotechnology, Vienna, Austria) for help with preparing the figures.

References

[1] A.-E. Saliba, I. Vonkova, A.-C. Gavin, The systematic analysis of protein-lipid interactions comes of age., Nat. Rev. Mol. Cell Biol. 16 (2015) 753–61. doi:10.1038/nrm4080.

[2] T.M. Allen, P.R. Cullis, Drug Delivery Systems: Entering the Mainstream, Science (80-.). 303 (2004) 1818–1822. doi:10.1126/science.1095833.

[3] D. Jeschek, G. Lhota, J. Wallner, K. Vorauer-Uhl, A versatile, quantitative analytical method for pharmaceutical relevant lipids in drug delivery systems, J. Pharm. Biomed. Anal. 119 (2016) 37–44. doi:10.1016/j.jpba.2015.11.020.

[4] H.H. Shen, T. Lithgow, L.L. Martin, Reconstitution of membrane proteins into model membranes: Seeking better ways to retain protein activities, Int. J. Mol. Sci. 14 (2013) 1589–1607. doi:10.3390/ijms14011589.

[5] V.L. C. Peetla, A. Stine, Biophysical interactions with model lipid membranes: applications in drug discovery and drug delivery, Mol Pharm. 6 (2009) 1264–1276. doi:10.1021/mp9000662.Biophysical.

[6] H. Shibata, H. Yoshida, K.I. Izutsu, Y. Haishima, T. Kawanishi, H. Okuda, Y. Goda, Interaction kinetics of serum proteins with liposomes and their effect on phospholipase-induced liposomal drug release, Int. J. Pharm. 495 (2015) 827–839. doi:10.1016/j.ijpharm.2015.09.053.

[7] J. Wallner, G. Lhota, D. Jeschek, A. Mader, K. Vorauer-Uhl, Application of Bio-Layer Interferometry for the analysis of protein/liposome interactions., J. Pharm. Biomed. Anal. 72 (2013) 150–4. doi:10.1016/j.jpba.2012.10.008.

[8] M. Beseničar, P. Maček, J.H. Lakey, G. Anderluh, Surface plasmon resonance in protein-membrane interactions, Chem. Phys. Lipids. 141 (2006) 169–178. doi:10.1016/j.chemphyslip.2006.02.010.

[9] Y. Abdiche, D. Malashock, A. Pinkerton, J. Pons, Determining kinetics and affinities of protein interactions using a parallel real-time label-free biosensor, the Octet, Anal. Biochem. 377 (2008) 209–217. doi:10.1016/j.ab.2008.03.035.

[10] K. Sou, T. Endo, S. Takeoka, E. Tsuchida, Poly(ethylene glycol)-Modification of the Phospholipid Vesicles by Using the Spontaneous Incorporation of Poly(ethylene glycol)-Lipid into the Vesicles, Bioconjug. Chem. 11 (2000) 372–379. doi:10.1021/bc990135y.

[11] S.C. Owen, D.P.Y. Chan, M.S. Shoichet, Polymeric micelle stability, Nano Today. 7 (2012) 53–65. doi:10.1016/j.nantod.2012.01.002.

[12] L. Vukovi, F.A. Khatib, S.P. Drake, A. Madriaga, K.S. Brandenburg, Structure and Dynamics of Highly PEG-ylated Sterically Stabilized Micelles in Aqueous Media Petr Kr, J. Am. Chem. Soc. 133 (2011) 13481–13488.

[13] Y.L. Lo, Y.E. Rahman, Protein location in liposomes, a drug carrier: a prediction by differential scanning calorimetry., J. Pharm. Sci. 84 (1995) 805–14. http://www.ncbi.nlm.nih.gov/pubmed/7562428 (accessed 24 November 2016).

[14] A.D. Bangham, M.M. Standish, J.C. Watkins, Diffusion of univalent ions across the lamellae of swollen phospholipids., J. Mol. Biol. 13 (1965) 238–252. doi:10.1016/S0022-2836(65)80093-6.

[15] A.A. Spector, M.A. Yorek, Membrane lipid composition and cellular function., J. Lipid Res. 26 (1985) 1015–35. doi:3906008.

[16] P. Kuhn, K. Eyer, T. Robinson, F.I. Schmidt, J. Mercer, P.S. Dittrich, A facile protocol for the immobilisation of vesicles, virus particles, bacteria, and yeast cells., Integr. Biol. (Camb). 4 (2012) 1550–5. doi:10.1039/c2ib20181j.

[17] F. Olson, C.A. Hunt, F.C. Szoka, W.J. Vail, D. Papahadjopoulos, Preparation of liposomes of defined size distribution by extrusion through polycarbonate membranes, BBA - Biomembr. 557 (1979) 9–23. doi:10.1016/0005-2736(79)90085-3.

[18] G. van Meer, D.R. Voelker, G.W. Feigenson, Membrane lipids: where they are and how they behave., Nat. Rev. Mol. Cell Biol. 9 (2008) 112–124. doi:10.1038/nrm2330.

[19] P.S. Katsamba, I. Navratilova, M. Calderon-Cacia, L. Fan, K. Thornton, M. Zhu, T. Vanden Bos, C. Forte, D. Friend, I. Laird-Offringa, G. Tavares, J. Whatley, E. Shi, A. Widom, K.C. Lindquist, S. Klakamp, A. Drake, D. Bohmann, M. Roell, L. Rose, J. Dorocke, B. Roth, B. Luginbühl, D.G. Myszka, Kinetic analysis of a high-affinity antibody/antigen interaction performed by multiple Biacore users, Anal. Biochem. 352 (2006) 208–221. doi:10.1016/j.ab.2006.01.034.

[20] C. Bee, Y.N. Abdiche, D.M. Stone, S. Collier, K.C. Lindquist, A.C. Pinkerton, J. Pons, A. Rajpal, Exploring the Dynamic Range of the Kinetic Exclusion Assay in Characterizing Antigen-Antibody Interactions, PLoS One. 7 (2012) e36261. doi:10.1371/journal.pone.0036261.

[21] Y.N. Abdiche, D.S. Malashock, J. Pons, Probing the binding mechanism and affinity of tanezumab, a recombinant humanized anti-NGF monoclonal antibody, using a repertoire of biosensors., Protein Sci. 17 (2008) 1326–35. doi:10.1110/ps.035402.108.

[22] J. Wallner, M. Kühleitner, N. Brunner, G. Lhota, K. Vorauer-Uhl, Application of the log-normal model for long term high affinity antibody/antigen interactions using Bio-Layer Interferometry, J. Math. Chem. 52 (2014) 575–587. doi:10.1007/s10910-013-0278-9.

[23] G. Stepanov, O. Gnedenko, A. Mol'nar, A. Ivanov, Y. Vladimirov, A. Osipov, Evaluation of cytochrome *c* affinity to anionic phospholipids by means of surface plasmon resonance, FEBS Lett. 583 (2009) 97–100. doi:10.1016/j.febslet.2008.11.029.

[24] D.A. Armbruster, T. Pry, Limit of blank, limit of detection and limit of quantitation., Clin. Biochem. Rev. 29 Suppl 1 (2008) S49-52. http://www.ncbi.nlm.nih.gov/pubmed/18852857 (accessed 24 November 2016).

[25] M. a Cooper, a Hansson, S. Löfås, D.H. Williams, A vesicle capture sensor chip for kinetic analysis of interactions with membrane-bound receptors., Anal. Biochem. 277 (2000) 196–205. doi:10.1006/abio.1999.4389.

[26] R. Tanaka, R. Gomi, K. Funasaka, D. Asakawa, H. Nakanishi, H. Moriwaki, Development of a novel evaluation method for air particles using surface plasmon resonance spectroscopy analysis., Analyst. 138 (2013) 5437–43. doi:10.1039/c3an00704a.

[27] M. Beseničar, P. Maček, J.H. Lakey, G. Anderluh, Surface plasmon resonance in protein–membrane interactions, Chem. Phys. Lipids. 141 (2006) 169–178. doi:10.1016/j.chemphyslip.2006.02.010.

[28] T.M. Allen, P. Sapra, E. Moase, Use of the post-insertion method for the formation of ligand-coupled liposomes., Cell. Mol. Biol. Lett. 7 (2002) 889–894. http://www.ncbi.nlm.nih.gov/pubmed/12378272.

[29] A. Holmberg, A. Blomstergren, O. Nord, M. Lukacs, J. Lundeberg, M. Uhlén, The biotin-streptavidin interaction can be reversibly broken using water at elevated temperatures, Electrophoresis. 26 (2005) 501–510.

doi:10.1002/elps.200410070.
[30] H. Bakowsky, T. Richter, C. Kneuer, D. Hoekstra, U. Rothe, G. Bendas, C. Ehrhardt, U. Bakowsky, Adhesion characteristics and stability assessment of lectin-modified liposomes for site-specific drug delivery, Biochim. Biophys. Acta - Biomembr. 1778 (2008) 242–249. doi:10.1016/j.bbamem.2007.09.033.
[31] J.N. Israelachvili, Intermolecular and Surface Forces Third Edition, 2010. doi:10.1016/B978-0-12-375182-9.10025-9.
[32] C. Thévenot, B. Grassl, G. Bastiat, W. Binana, Aggregation number and critical micellar concentration of surfactant determined by time-dependent static light scattering (TDSLS) and conductivity, Colloids Surfaces A Physicochem. Eng. Asp. 252 (2005) 105–111. doi:10.1016/j.colsurfa.2004.10.062.
[33] Y. Hong, J. Muenzner, S.K. Grimm, E. V. Pletneva, Origin of the Conformational Heterogeneity of Cardiolipin-Bound Cytochrome *c*, J. Am. Chem. Soc. 134 (2012) 18713–18723. doi:10.1021/ja307426k.
[34] H. Zhao, P. Lappalainen, A simple guide to biochemical approaches for analyzing protein-lipid interactions., Mol. Biol. Cell. 23 (2012) 2823–30. doi:10.1091/mbc.E11-07-0645.
[35] G. Anderluh, M. Beseničar, A. Kladnik, J.H. Lakey, P. Maček, Properties of nonfused liposomes immobilized on an L1 Biacore chip and their permeabilization by a eukaryotic pore-forming toxin, Anal. Biochem. 344 (2005) 43–52. doi:10.1016/j.ab.2005.06.013.

Highligths

Liposome/protein interaction assay with Bio-layer Interferometry was developed.

DSPE-$PEG_{(2000)}$-biotin was formulated as stabilized micelles (SSMs).

SSMs were used as precursors to immobilize intact liposomes.

Liposomes of various compositions were immobilized.

Immobilized liposomes were used for protein interaction studies.